Energy, Ecology and Environment (2024) 9(3):256–271
https://doi.org/10.1007/s40974-023-00309-1

ORIGINAL ARTICLE

Evaluation of strength and durability properties of fly ash-based geopolymer concrete containing GGBS and dolomite

Mansi Thakur[1] · **Shailja Bawa**[1]

[1] Department of Civil Engineering, Dr B R Ambedkar National Institute of Technology, Jalandhar, Punjab 144011, India

Received: 11 March 2023 / Revised: 3 December 2023 / Accepted: 4 December 2023 / Published online: 29 December 2023

Abstract Ordinary Portland cement is a construction material that is widely utilized all over the world. Aside from deforestation and fossil fuel combustion, the cement manufacturing industry contributes significantly to carbon dioxide emissions, which questions the viability of using Portland cement (PC) in concrete construction. Therefore, finding an alternative to the existing one becomes crucial. Geopolymer concrete (GPC) is a relatively advanced and innovative form of concrete that can be prepared without the use of PC. The present research emphasizes the assessment of the strength and durability of GPC containing fly ash (FA), ground-granulated blast furnace slag (GGBS), and dolomite as binders. The control mix consists entirely of FA as a binder, while five additional mixes are prepared by replacing 20% FA with either GGBS or dolomite or in varying combinations. The slump test is used to assess the workability of the concrete. Key mechanical properties such as compressive strength and split tensile strength are also determined, along with non-destructive tests including ultrasonic pulse velocity and electrical resistivity. To assess GPC durability, initial surface absorption and capillary suction absorption tests are conducted at various curing ages. The findings demonstrate that incorporating GGBS and dolomite into FA-based GPC results in notable improvements in both strength and durability. However, this enhancement reduces the workability compared to the control mix. The addition of GGBS and dolomite yields remarkable enhancements in compressive strength, showing an impressive surge of up to 67%, and a substantial reduction in initial surface absorption, up to 65%, as compared to the control mix over a period of 56 days. The most favorable results in terms of both strength and durability are achieved when FA is replaced with 20% of GGBS. Also, the mix containing a combination of 10% GGBS and 10% dolomite yields comparable results to the mix with 20% GGBS, making it a cost-effective alternative.

✉ Mansi Thakur
mansithakur199740@gmail.com

Shailja Bawa
bawas@nitj.ac.in

Graphical abstract

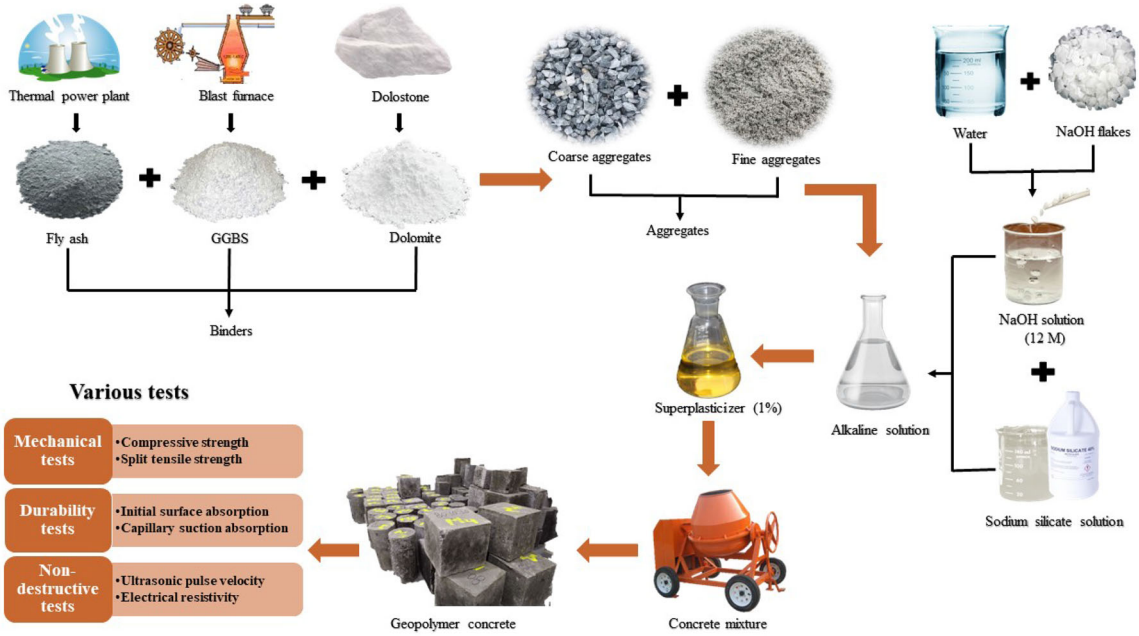

Keywords Fly ash · GGBS · Dolomite · Alkaline activators · Geopolymer concrete

1 Introduction

In recent years, significant advancements have been made in various fields toward achieving sustainability and combating climate change (Gandolfo et al. 2022). These advancements extend to key sectors such as construction, transportation, and energy production, which play crucial roles in the global pursuit of sustainability. The escalating industrialization, rapid population growth, and technological advancements of the past few decades have led to increased energy consumption (Adediji et al. 2023). The construction sector, for instance, is now recognized as a vital player in the fight against climate change, as it accounts for nearly 40% of CO_2 emissions (Švajlenka and Pošiváková 2023). The sustainable development of the construction sector, which accounts for significant resource consumption, electrical power usage, water consumption, landfill waste generation, and greenhouse gas emissions, is of paramount importance in the pursuit of sustainability. Concrete, as a widely used material, poses challenges due to non-renewable raw materials and their ecological footprint during production (Fonseca and Matos 2023). Another critical aspect in the transition toward sustainability is the transformation of the energy production sector, with a focus on cleaner and renewable energy sources. Photovoltaics, including Si and multijunction solar cells, have demonstrated remarkable efficiency values, showcasing their potential to significantly contribute to sustainable energy generation (Pirrone et al. 2022). Additionally, utilizing carbon materials derived from the hydrothermal recycling of waste tires highlights the importance of end-of-life waste management (Schmitz et al. 2022). The global population is projected to increase to approximately 9.8 billion by 2050; hence, there is a growing demand for sustainable solutions (Eisa et al. 2022). This necessitates rethinking traditional construction materials and processes to meet the needs of the future, while minimizing resource consumption and greenhouse gas emissions.

The rise in urbanization has led to the emergence of the building and construction sector, which in turn has raised the demand for cement (Singh et al. 2022). OPC has long been used as the primary binding material in the production of concrete, but the environmental concerns associated with its production are well known. A substantial amount of CO_2 is emitted due to the calcination of limestone and the burning of fossil fuels during OPC production (Liu et al. 2016; Singh and Subramaniam 2019). Furthermore, the calcination of lime requires temperatures of about 1400–1500 °C, which deplete a lot of natural resources and use a substantial amount of energy (Thakur and Bawa 2022). Globally, the cement industry is liable for 5–8% of all CO_2 emanations (Kajaste and Hurme 2016; Farooq et al. 2022). A rough estimate suggests that carbon fuel combustion results in about 0.40 tons of CO_2 emissions, while 0.55 tons of chemical CO_2 are released during the

processing of 1 ton of Portland clinker. On simplification, around 1 ton of CO_2 is generated in general (Davidovits 1994; Sharma et al. 2022a). CO_2 is the most significant greenhouse gas contributor, responsible for about 65% of the warming effect. It is estimated that OPC production contributes around 1.35 billion tons per year to global greenhouse gas emissions (Malhotra 2002). Materials like FA, wood ash, GGBS, silica fume, rice husk ash, and other low-energy, low-carbon products are viable alternatives for addressing this issue (Nath and Sarker 2015; Pasupathy et al. 2017).

GPC is considered a revolutionary development in the world of concrete technology. When compared to traditional cement, the production of geopolymer cement results in a reduction of CO_2 emissions up to 80% by eliminating the need for calcium carbonate (Junaid et al. 2017). Geopolymer cement cures more quickly than Portland-based cement. The majority of their strength is attained within 24 h (Davidovits 2013). GPC outperforms normal concrete in terms of mechanical and thermal aspects (Zhao et al. 2019; Qu et al. 2020). This concrete is an environmental friendly and sustainable alternative to traditional PC concretes (Ambikakumari Sanalkumar and Yang 2021; Gill et al. 2023). GPC shows high durability with the ability to resist chloride penetration and acid attack, which are some of the basic requirements for durable performance (Radahakrishnan et al. 2017). Davidovits, in 1978, suggested that binders could be developed by a polymeric reaction of alkaline solutions with aluminum (Al) and silicon (Si) in geologically derived primary sources or industrial by-products such as FA, GGBS, and so on (Davidovits 1999; Provis 2014). These Si and Al are polymerized into molecular chains and used as binders after being dissolved in an alkaline activating solution (Abdul Aleem and Arumairaj 2012). Geopolymerization is a process that involves a heterogeneous reaction between alkali metal silicate solution and aluminosilicate oxides at mild temperatures and high alkalinity to produce a polymeric structure that is either amorphous or semi-crystalline in nature, with Si–O–Al and Si–O–Si bonds (Dimas et al. 2009).

FA disposal is becoming increasingly difficult, with only 15% of FA now being used for high-value-added uses, such as concrete construction, and the rest is being used as landfills. FA is effectively used in cement concrete production because it provides technical benefits while also decreasing pollutants (Howladar and Islam 2016; Bhatt et al. 2019). GGBS is extremely cementitious and rich in calcium silicate hydrates (CSH) that enhance the strength, durability, and aesthetic quality of concrete (Patel and Shah 2018). Therefore, there is a pressing need to encourage the use of GGBS due to its extensive benefits. The addition of limestone powder, dolomite, or quick lime to GGBS can intensify the Ca–OH bonds, which enhance the early-age strength of the concrete without altering its pH (Saranya et al. 2019). Dolomite, also referred to as calcium magnesium carbonate ($CaMg(CO_3)_2$), is a type of carbonate mineral obtained by grinding sedimentary rock to produce the mineral dolostone. Due to its superior surface hardness, density, high purity, flame-retardant properties, good compression strength, weathering resistance, and shearing characteristics, dolomite is a desirable construction material (Barbhuiya 2011; Agrawal et al. 2021). Geopolymerization of Class F FA requires some constraints, such as the application of exogenous heat or the presence of calcium content, to speed up the chemical reactions involved (Nath and Sarker 2015; Sharma et al. 2022b). Various studies suggest that adding high-calcium components to FA-based geopolymers significantly increases their strength properties (Yip et al. 2005; Cohen et al. 2019). The amount and source of calcium in the FA influences the characteristics of the resultant geopolymer. The existence of calcium compounds in the raw material can enhance the mechanical characteristics of the geopolymers due to the cohabitation of the geopolymeric gel and the calcium aluminum hydrate (CAH) and calcium silicate hydrate (CSH) gels (Yip et al. 2005; Buchwald et al. 2007). GGBS and dolomite are rich in calcium (Ca) content and hence can be used with geopolymer binder to improve the strength and durability of the GPC.

2 Research significance

Solid waste disposal has become the world's top environmental priority. Waste products geopolymerization can assist in the resolution of current environmental issues such as water, soil, and air pollution (Thakur and Bawa 2022). On the contrary, the construction industry contributes significantly to environmental pollution, particularly through the manufacture of its most widely used product, cement (Ahmed et al. 2022; Wong 2022). As a result, achieving sustainability in the construction industry has become critical, and this research is a step forward in terms of sustainable development and natural resource optimization. With the use of FA, GGBS, which are industrial by-products, and dolomite, which is a low-cost material, two very major problems of this time, i.e., safe discarding of industrial wastes and minimization of environmental pollution by the construction industry, can be handled (Prabha et al. 2022; Asghar et al. 2023). Previous studies have extensively explored the use of either FA or GGBS as cementitious binders in GPC (Pasupathy et al. 2017; Reddy et al. 2018; Qu et al. 2020; Sharma et al. 2022b). However, limited attention has been given to the incorporation of dolomite. Dolomite is a low-cost material that can be sourced easily, making it an economically viable option for

GPC production (Prabha et al. 2022). This investigation aims to explore the potential benefits of incorporating dolomite in a ternary blend of FA, GGBS, and dolomite as binders in GPC and assess their compatibility, which has not been previously studied. Additionally, the research emphasizes studying and quantifying the benefits obtained, on the mechanical and durability aspects of the developed GPC. By assessing the ternary blend performance, in terms of strength, durability, and other relevant properties, this research provides valuable insights into the potential advantages and limitations of using these materials in combination.

Table 1 Physical and chemical properties of FA, GGBS, and dolomite

Chemical compounds (%)	FA	GGBS	Dolomite
Al_2O_3	33.9	18.2	8.36
SiO_2	54.5	33.1	20.84
Fe_2O_3	4.2	0.31	2.67
CaO	3.1	35.3	34.35
MgO	2.3	7.6	21.57
LOI	1.3	0.26	11.09
Physical properties			
Fineness (cm^2/g)	3900	4025	–
Specific gravity	2.14	2.85	2.82

3 Experimental program

3.1 Materials

The materials used for the manufacturing of FA-based GPC were low-calcium FA (Class F), GGBS, dolomite, aggregates, alkaline activators, and superplasticizer (SP). Class F FA was the principal binder in all the GPC mixes, and it was blended with GGBS and dolomite in different proportions. The control GPC mix used in this investigation was made using 100% FA, coarse aggregate, fine aggregate, alkaline solution, and SP. For the remaining mixes, the total cementitious content of the control GPC mix was modified by replacing FA up to 20% with GGBS and dolomite in various percentages. FA used in the manufacturing process was collected from a thermal power plant, Rajpura, in accordance with IS 3812 (Part-1) (2003). GGBS conforming to IS 12089 (1987) and dolomite passing through 75 µm were also utilized in the production of GPC, both of which were obtained from a nearby chemical mill and store. The physical and chemical properties of FA, GGBS, and dolomite are illustrated in Table 1. Locally available fine aggregates comprising river sand with a maximum particle size of around 4.75 mm, specific gravity of 2.62, and fineness modulus of 2.99 conforming grading zone II as per IS 383–2016 (Standard 2016) were used. Coarse aggregates having specific gravity of 2.68 and fineness modulus of 7.08 were used in accordance with IS 383–2016 (Standard 2016). The aggregates passing through a 12.5-mm sieve and retained on a 10-mm sieve and aggregates passing through a 10-mm sieve and retained on a 4.75-mm sieve were utilized in proportions of 40:60, respectively. Figure 1 represents the gradation curve for both fine and coarse aggregates. Blend of sodium

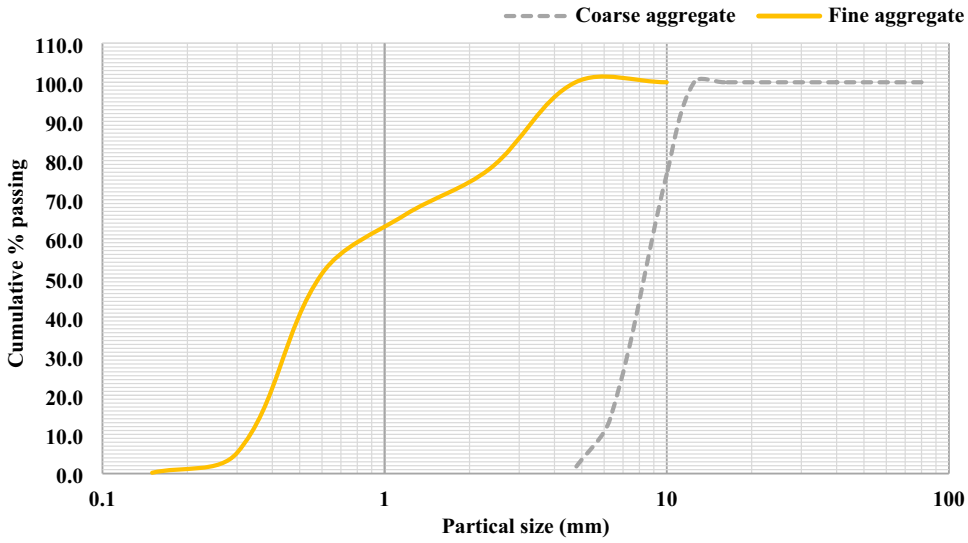

Fig. 1 Fine and coarse aggregates gradation curve

Table 2 Mixes nomenclature

S. no.	Mix ID	Mix description
1	FA100	Control mix with 100% FA, 0% GGBS, 0% dolomite
2	G20D0	Mix with 80% FA, 20% GGBS, 0% dolomite
3	G15D5	Mix with 80% FA, 15% GGBS, 5% dolomite
4	G10D10	Mix with 80% FA, 10% GGBS, 10% dolomite
5	G5D15	Mix with 80% FA, 5% GGBS, 15% dolomite
6	G0D20	Mix with 80% FA, 0% GGBS, 20% dolomite

Table 3 Quantity of various binders used for each mix preparation in kg/m^3

S. no.	Mix ID	FA	GGBS	Dolomite	Fine aggregates	Coarse aggregates	NaOH	Na_2SiO_3	SP
1	FA100	450	–	–	760.16	912.79	67.5	135	4.5
2	G20D0	360	119.86	–	760.16	912.79	67.5	135	4.5
3	G15D5	360	89.89	29.65	760.16	912.79	67.5	135	4.5
4	G10D10	360	59.93	59.29	760.16	912.79	67.5	135	4.5
5	G5D15	360	29.96	88.95	760.16	912.79	67.5	135	4.5
6	G0D20	360	–	118.59	760.16	912.79	67.5	135	4.5

silicate (Na_2SiO_3) and sodium hydroxide (NaOH) solution was preferred as an alkaline solution. Na_2SiO_3 with a specific gravity of 1.53 and SiO_2/Na_2O ratio of 1.5 and NaOH with a specific gravity of 1.33 and 12 M concentration were used during the manufacturing process. The hydroxide to silicate ratio was maintained at 1:2. A commercial grade Na_2SiO_3 solution and NaOH flakes were acquired from a nearby supplier. The NaOH solution was prepared 24 h before casting by dissolving 98% pure solid flakes in water. Since the dissolution of NaOH flakes into the water is an exothermic reaction, it requires 24 h to attain the room temperature. Na_2SiO_3 was added to this NaOH solution just half an hour before mixing. The viscosity of the alkaline solution is greater than that of potable water. When these alkaline solutions are employed in the production of GPC, they tend to hinder the workability of the concrete (Pavithra et al. 2016). Therefore, a polycarboxylic ether-based SP was utilized to enhance workability and retain the desired slump value of the concrete mixture.

3.2 GPC mix proportions

In total, six mixes were formulated at varying percentages of FA, GGBS, and dolomite. Mix with 100% FA was used as a reference mix or control mix. For all mixture designs, a constant alkali/binder ratio (a/b) of 0.45 and binder content of 450 kg/m^3 were utilized. Combination of Na_2SiO_3 and NaOH solution with silicate to hydroxide ratio of 2 (Na_2SiO_3 / NaOH) was used as an alkaline solution for activation, and the concentration of NaOH solution was maintained as 12 M. The SP proportion was held constant at 1% of binder for all mixes. Table 2 enlists the nomenclature of various GPC mixes, and Table 3 demonstrates the mix proportion of all GPC mixes. Due to the lack of standardized guidelines for GPC, the mix design procedure adopted in this study was inspired by prior research done on FA-based GPC. The basic mix proportion for the control mix was taken from the previous studies (Patankar et al. 2015; Pavithra et al. 2016; Reddy et al. 2018). The preparation of the GPC mixes was done in two stages. Firstly, the binders were mixed thoroughly with coarse aggregates and sand in saturated surface dry condition for 5 min in a tilting-type power-operated rotary concrete mixer before. After that, an alkaline solution and SP were added gradually to this dry mix of binder, coarse, and fine aggregates and further mixed to ensure a uniform consistency of the mix. Finally, the fresh GPC mix was poured into the molds and secured with the poly wrap to prevent moisture loss. After casting, all samples were labeled with their corresponding mix designations and oven-cured at 65 °C for 24 h before being demolded.

3.3 Workability

3.3.1 Slump test

The slump test examines the consistency of freshly prepared concrete prior to its hardening and also tells about the amount of water required for achieving a desired workability. The slump test for all the mixes was performed in accordance with IS 1199 (1959). The SP dosage was kept

constant (1% of binder) throughout the experiment, and the slump value was measured.

3.4 Mechanical strength tests

3.4.1 Compressive strength

The compressive strength testing was performed conforming to Indian Standard IS 516 (1959). Cubes measuring 100 mm * 100 mm * 100 mm were cured for 7, 28, and 56 days, and then tested for compressive strength.

3.4.2 Split tensile strength

The split tensile strength of GPC mixes was conducted in accordance with IS 5816 (1999). The 100 * 200 mm cylindrical specimens were prepared for testing the split tensile strength at 7, 28, and 56 days of curing.

3.5 Durability tests

3.5.1 Initial surface absorption (ISA)

Initial surface absorption test (ISAT) provides a low-pressure assessment of the concrete surface water absorption. This test examines the rate of water flow into a concrete capillary pore network. Flow volume is measured by computing the length of flow along a known dimension capillary. The ISA of GPC was determined by testing 150 mm*150 mm*150 mm cube specimens at 28 and 56 curing days confirming to BS 1881–208 (1996). Specimens were subjected to oven drying to achieve a consistent weight (i.e., not more than 0.1% weight variation during any 24-h drying period) prior to the test and placed in a cooling cabinet (desiccator) at the temperature of 20 °C to cool them to the room temperature. For each type of concrete mix and each curing age, three distinct specimens were evaluated. A gasketed circular cap with the smallest surface area of 5000 mm^2 is sealed to the concrete surface in the test technique. The cap outflow is attached to a capillary tube, and the cap is filled with deionized water from a reservoir. After isolating the reservoir, the displacement of a meniscus along the capillary tube is measured to estimate the rate of water absorption into the concrete at 200-mm pressure head. Readings are noted at 10 min, 30 min, and 60 min.

3.5.2 Capillary suction absorption (CSA)

Capillary suction absorption test (CSAT) determines the water absorption rate of concrete by monitoring the increase in mass of a specimen as a function of time when only one surface of the sample is immersed in water. A small amount of capillary suction is responsible for most of the unsaturated concrete water infiltration at the first contact with water. In unsaturated concrete, capillary rise is a major factor in the pace at which water or other liquids may enter the concrete. In this test, the exposed side of the concrete capillary pores is examined for water infiltration and the results are recorded. Three discs, each 50 mm thick and 100 mm in diameter, were used and conditioned in accordance with ASTM C1585-13 (2013) and aged for 28 and 56 days before testing. When the mass variation of the succeeding two measurements of the sample fell below 0.1%, the sample was put in a desiccator to cool down and prevent moisture absorption from the environment after oven drying at 105 °C. The circumferential area of the disc was covered with epoxy and sealed with polyethene sheets to avoid evaporation from the surface that was not exposed to water. Before immersing the specimens in water over a support, their mass was recorded. The mass of the samples was measured at intervals of 1, 5, 10, 20, 30, 60 min, and every hour up to 6 h. After the first 6 h, we took readings once a day for the next three days, then three readings at least 24 h apart for days four to seven, and a final reading at least 24 h after the reading on day seven. The sorptivity (mm/s) of the mixtures was determined by plotting the correlation between water absorption and the square root of time.

3.6 Non-destructive tests

3.6.1 Ultrasonic pulse velocity (UPV)

According to the UPV test method recommended by IS 516: Part 5 (2018), 100 mm * 100 mm * 100 mm cube specimens were tested on 7, 28, and 56 curing days prior to a compression test. This test instrument comes with a pulse generator, a set of two transducers in which one is a pulse emitter and the other is a receiver, and an electronic timing gadget. An ultrasonic pulse was induced into the cube specimen using an electro-acoustical transducer to determine internal cracks, defects, and homogeneity of the concrete mix. In order to further define the quality of the concrete, the time taken by the pulse wave to travel through the concrete specimens was precisely measured. Prior to pulse transmission, ultrasound gel was properly applied to any parallel sides of the cube except the casting side to properly transmit the electronic pulse from the specimen.

3.6.2 Electrical resistivity

All cylindrical specimens of 100 mm * 200 mm size were tested for electrical resistivity on 7, 28, and 56 curing days before their split tensile testing as per the electrical

resistivity test method recommended by AASHTO–T 358 (2015). Four uniformly spaced (1.5 in.) probes are applied to the specimen in a line in this procedure. The current is supplied to the specimen via the two outer probes, and the inner pair of electrodes monitors the resulting potential drop. All of the probes are used on the same surface of the specimen. This test assesses the resistance of concrete to chloride ion penetration.

3.7 ANOVA test

A one-way ANOVA test was conducted, at a significance level of 5%, to examine the combined effect of all binders on the mechanical properties. The design specifications to perform one-way ANOVA are:

- Each dataset is based on the number of days of curing at 7, 28, and 56 days, respectively.
- The six mixes under consideration are FA100, G20D0, G15D5, G10D10, G5D15, and G0D20.
- At 5% level of significance, the hypothetical statements under consideration are:

H_0: There is no significant difference between the six sets of mixes for given number of days versus H_1: There is some remarkable difference between the six sets of mixes for given number of days.

3.8 Reliability of strength

The significant variation in the mechanical strength at 7, 28, and 56 curing days, due to the inclusion of different binders, was further studied for its reliability. To assess the reliability of strength, a regression analysis was conducted using different percentages of GGBS and dolomite. The analysis focuses on exploring the R^2 value, standard error, P value, and T statistics.

4 Results and discussion

The current investigation analyzed the effect of inclusion of GGBS and dolomite on both the strength and durability properties of GPC at temperature curing. Prior to the casting stage, the fresh property of GPC was examined by measuring the slump value. The strength properties in terms of compressive strength and split tensile strength, durability properties of GPC mixes such as ISA and CSA, and non-destructive tests such as UPV and electrical resistivity were evaluated. The outcomes of various tests performed are discussed below:

4.1 Slump test

The purpose of the test is to determine the workability of freshly prepared concrete. The desired workability parameter, in terms of slump value, has been achieved for each mix, as all concrete mixtures demonstrated slump in the 35–75-mm range. However, the mixes G20D0, G15D5, G10D10, G5D15, and G0D20, which were prepared with the inclusion of GGBS and dolomite, resulted in a 34.24%, 39.72%, 42.46%, 46.57%, and 49.31% reduction in the slump value when compared with the control mix FA100 (73 mm). The mixes with the higher percentages of GGBS and dolomite were stickier and cohesive. Due to the unsymmetrical particle shape and finer particle size of GGBS and dolomite compared to FA particles, these binders possess greater specific surface area, which elevates the water requisite of the GPC mix and reduces its workability. Low fluidity and flowability of the GPC mixtures have been observed where higher amounts of dolomite proportions were used due to higher water absorption than GGBS. The previous studies on GPC containing FA, GGBS, and dolomite also reported similar findings, indicating that both GGBS and dolomite possess irregular shapes (Ibrahim et al. 2022; Singh et al. 2023) and significantly finer particle sizes compared to FA (Ye et al. 2019; Liang et al. 2022). Additionally, it has been observed that the particle size of dolomite is even finer than that of slag (Ye et al. 2019). Figure 2 summarizes the slump values for different mixes.

4.2 Compressive strength

Compressive strength of concrete is of immense value and is the measure of the amount of compressive load a concrete sample can bear. It is a reflecting and a realistic indicator for evaluating the overall performance of any concrete structure. The result of compressive strength tests

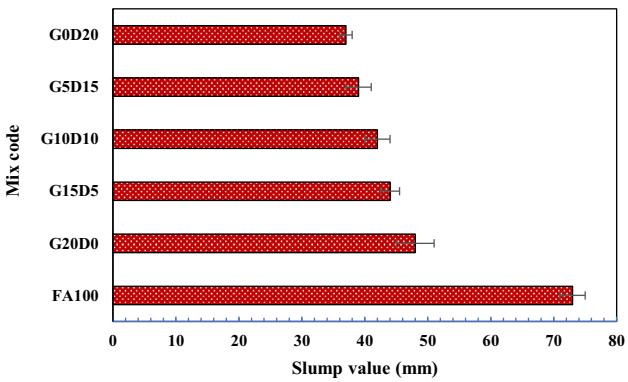

Fig. 2 Slump test results

shows that the inclusion of GGBS and dolomite as partial replacement of FA enhances the compressive strength of the concrete mixes. The mixes G20D0 and G10D10 show the maximum compressive strength values. Hence, the following sequence has been suggested for the GPC mixes based on the compressive strength test results: G20D0 > G10D10 > G15D5 > G5D15 > G0D20 > FA100. All GGBS and dolomite-blended mixes resulted in better compressive strength than the control mix FA100 at all mentioned curing days. As a result, there is an increment of nearly 53.21%, 35.47%, 48.28%, 32.02%, and 10.35% for the mixes G20D0, G15D5, G10D10, G5D15, and G0D20, respectively, compared to control mix FA100 (20.3 MPa) at 7 days of curing. Also, with the increase in curing days, the compressive strength improved for all GPC mixes due to pozzolanic behavior, pore structure refinement, and formation of C–S–H gel. At 28 days of curing, strength gain of 28.5714%, 45.0161%, 31.2727%, 41.196%, 27.2388%, and 41.5179% has been observed as compared to strength at 7 days of FA100, G20D0, G10D10, G15D5, G5D15, and G0D20 mixes, respectively. Furthermore, at 56 days of curing, strength gain of 66.2%, 36.23%, 58.18%, 29.61%, and 19.51% was observed for the mixes G20D0, G15D5, G10D10, G5D15, and G0D20, respectively, when compared to the control mix FA100 (28.7 MPa). Also, it has been noticed that the compressive strength of G20D0 and G10D10 was comparable with each other at all curing ages. Increased calcium and silicate content in GGBS and dolomite leads to increased strength by increasing the hydration rate, and these two binders also have significantly distinct particle shapes and morphology than that of FA, i.e., spherical and smooth for FA and asymmetrical and rough for GGBS and dolomite, leading to superior mechanical characteristics in FA-based mixtures. The asymmetrical and complicated shape of the GGBS and dolomite particles results in mechanical anchoring within the concrete matrix, thus enhancing the hardened mixture compressive strength. Previous studies have also reported the positive effect of adding dolomite on compressive strength through two mechanisms: mechanical anchoring due to the differences in the particle shapes and morphologies of dolomite particles within the matrix, with FA, and enhanced hydration reaction (Cohen et al. 2019). Similarly, the angular shape of GGBS particles and the presence of calcium accelerate the reaction, leading to improved mechanical properties (Ramineni et al. 2018). Since the finer particles fill the voids and make the matrix dense, increasing the binder fineness results in a substantial enhancement in GPC strength. Figure 3 represents the results of the compressive strength tests conducted on the various mixes made with GGBS and dolomite as replacement of FA at 7, 28, and 56 days of curing period.

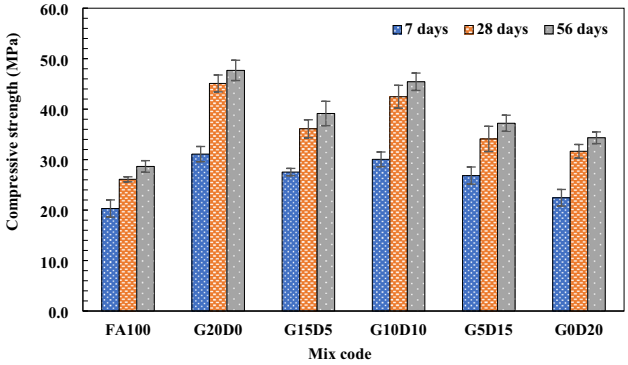

Fig. 3 Compressive strength values of different mixes at 7, 28, and 56 curing days

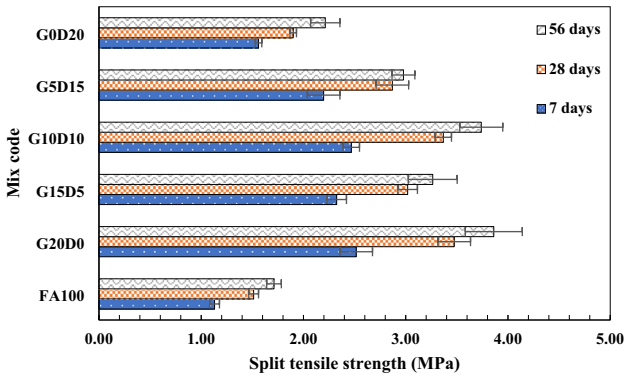

Fig. 4 Split tensile strength values of different mixes at 7, 28, and 56 curing days

4.3 Split tensile strength

The split tensile strength of FA-based GPC was tested on the specimens at the different ages of 7, 28, and 56 days to study the effect of GGBS and dolomite inclusion on it. The results of the split tensile strength test of the concrete at all ages are presented in Fig. 4, and it shows a similar trend to the results of compressive strength tests. The addition of GGBS and dolomite as partial replacements for FA improved the concrete mixes split tensile strength. The mixes G20D0 and G10D10 show the maximum split tensile strength values. As a result, the GPC mixes should be arranged in the same order as the compressive strength test results: G20D0 > G10D10 > G15D5 > G5D15 > G0D20 > FA100. At all curing days, the GGBS and dolomite-blended mixes have higher split tensile strength values than the control mix FA100. The mixes G20D0, G15D5, G10D10, G5D15, and G0D20 have a significant increase of nearly 123%, 105.31%, 118.58%, 94.69%, and 38.05%, respectively, when compared to the control mix FA100 (1.13 MPa) after 7 days of curing. Also, it has been observed that the split tensile strength of G20D0 and

G10D10 was comparable with each other at all curing ages. However, the split tensile strength of all GPC mixes has risen with curing time due to pozzolanic behavior, pore structure refinement, and the generation of new strength-imparting hydration products. Strength gains of 33.63%, 37.69%, 30.17%, 36.44%, 30.45%, and 21.79% have been observed after 28 days of curing when compared to the strength of FA100, G20D0, G10D10, G15D5, G5D15, and G0D20 mixes at 7 days. Furthermore, strength gains of 125.7%, 90.64%, 118.71%, 74.26%, and 29.24% were spotted for the mixes G20D0, G15D5, G10D10, G5D15, and G0D20, respectively, as compared to the control mix FA100 (1.71 MPa) at 56 days of curing. The split tensile strength of GPC is enhanced by increasing the fineness of the binder material, as the finer particles fill voids and make the concrete matrix dense. Moreover, the increased calcium and silicate content in GGBS and dolomite leads to increased split tensile strength.

4.4 Initial surface absorption

ISAT is used to calculate the flow of water into a dry, flat concrete surface. The absorption rate was estimated by measuring the uniaxial water penetration on the surface of the concrete specimens, which are often exposed to severe circumstances. The surface absorption resistance is a crucial parameter for predicting the durability of concrete. Figure 5a, b illustrates the absorption rates of the six mixes after 28 and 56 curing days. The G20D0 mix has been found to have the lowest absorption rate at both curing periods followed by the mixes G10D10, G15D5, G5D15, and G0D20, and the highest magnitude of absorption rate has been attained by the control mix FA100. The rate of absorption gradually reduces with the addition of GGBS and dolomite. The percentage of absorption rate reduction for mix G20D0 has been recorded to rise with advancing curing regime from 28 to 56 days, ranging from 45.26 to 50.62%, which is directly equivalent with G10D10 mix ranging from 40 to 38.27% with respect to the control mix (0.95–0.81 ml/m^2 s) for 10 min. Similarly, the absorption rate for G15D5, G15D5, and G0D20 reduces by 30.52%, 26.31%, and 12.63% when related to that of control mix FA100 (0.95 ml/m^2 s) for 10 min at 28 days of curing. Furthermore, reductions of 35.8%, 27.16%, and 12.34% were observed for G15D5, G15D5, and G0D20 mixes, respectively, at 56 curing days when compared to the control mix FA100 (0.81 ml/m^2 s) for 10 min. As the time passes, the absorption rate also declines. For all the mixes, the rate of absorption decreases at 30 min and further decreases at 60 min. The absorption rate reduces by 61.2% and 65% at 30 min and 60 min, respectively, for mix G20D0 and 47.76% and 60% for mix G10D10 at 56 curing days in contrast to the control mix (0.67–0.60 ml/m^2 s).

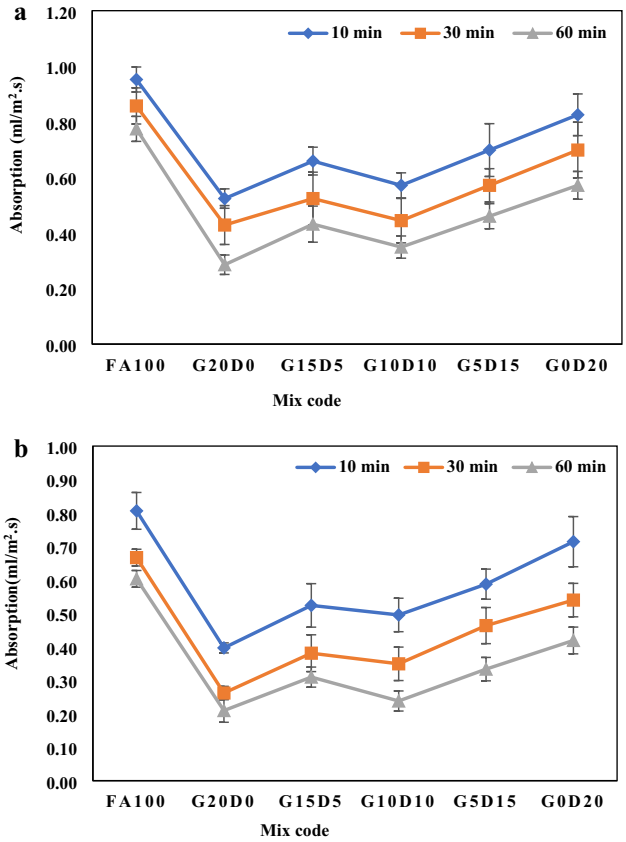

Fig. 5 **a** Initial surface absorption values after 28 days of curing. **b** Initial surface absorption values after 56 days of curing

Surface absorption is reduced due to the use of GGBS and dolomite because their finer particle size causes pore size refinement and thus makes the concrete matrix denser. Past studies have also indicated that the decrease in surface absorption can be ascribed to the finer characteristics of GGBS particles, which enhance the pore structure of concrete (Bostanci et al. 2016). Also, it has been observed that dolomite is even finer than that of GGBS (Ye et al. 2019), indicating that dolomite also possesses the capability to refine the pore structure, resulting in a denser matrix.

4.5 Capillary suction absorption

The sorptivity at early stages reveals the transport mechanism of the movement of water within concrete. It is evident from the findings that mix G20D0 has the lowest water absorption rate among all the mixes, followed by G10D10 mix. The initial rate of absorption (IRA) refers to the water absorption rate of GPC containing different proportions of binders for the first 6 h, while the secondary rate of absorption (SRA) is assessed over a period of 1–8 days. It can be observed that the rate of water absorption for all concrete becomes nearly stable after about 1 day. Figure 6a, b illustrates the combined value

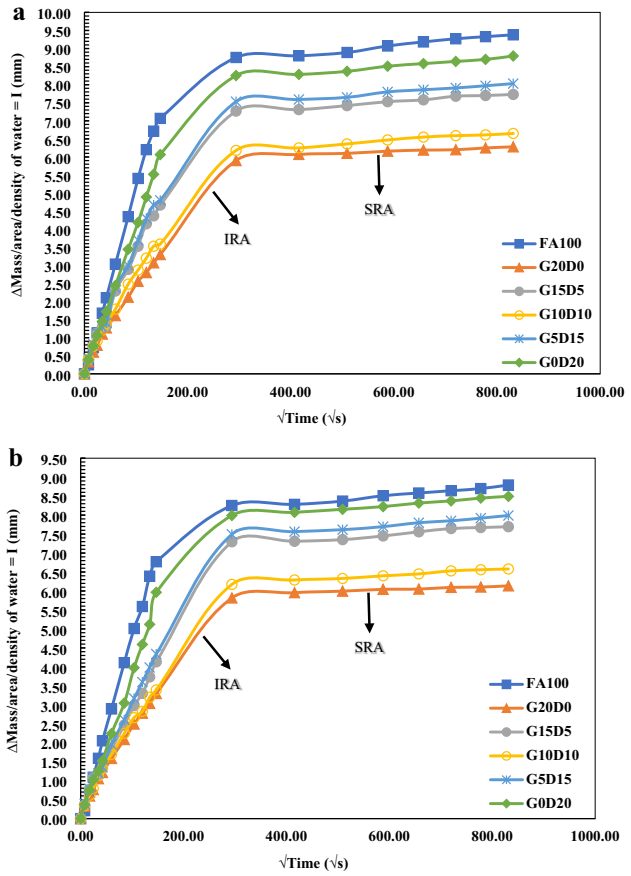

Fig. 6 **a** Capillary suction absorption values after 28 days of curing. **b** Capillary suction absorption values after 56 days of curing

(IRA + SRA) of capillary suction absorption after 28 and 56 curing days, respectively. The findings are also consistent with the initial absorption rate, as secondary absorption also decreases with the inclusion of GGBS and dolomite as a partial replacement of FA. The rate of initial absorption is about 57.19%, 37.47%, 52.27%, 34.71%, 19.92% lower for mixes G20D0, G15D5, G10D10, G5D15, G0D20, respectively, from that of control mix FA100 (0.0507 mm/s$^{1/2}$) at 28 curing days. The secondary absorption rate also decreases by 53.84%, 23.07%, 30.77%, 23.07%, 15.38% for mixes G20D0, G15D5, G10D10, G5D15, G0D20, respectively, from that of control mix FA100 (0.0013 mm/s$^{1/2}$) at 28 curing days. Similar trend has been observed for 56 curing days, and with the passage of time, the IRA and SRA values decrease for GPC. The decrease of 54.74%, 44.42%, 52.84%, 40.42%, and 18.31% in IRA and 54.54%, 18.18%, 27.27%, 18.18%, and 9.09% in SRA has been reported at 56 days of curing for mixes G20D0, G15D5, G10D10, G5D15, G0D20, respectively, from that of IRA-SRA of control mix FA100 (0.0475–0.0011 mm/s$^{1/2}$). The strength of concrete is significantly influenced by the water-to-cement ratio, which regulates air voids and thus secondary absorption. However, the initial absorption is governed by capillary forces (Albitar et al. 2017). Sorptivity proves that GGBS absorbs less water due to its crystalline structure (Purushotham et al. 2017). The finer particles of GGBS and dolomite result in the development of a dense microstructure that further reduces the IRA-SRA values.

4.6 Ultrasonic pulse velocity

Non-destructive testing is generally employed to examine the material integrity of the concrete structures. The UPV is an important non-destructive test which gives the impression about the quality of concrete. Greater the readings of pulse velocities, more is the quality of concrete. Inclusion of GGBS and dolomite increases the pulse velocity readings, and their addition in the concrete proves to be beneficial as the quality of concrete increases. Inclusion of these binders results in denser concrete as its finer particles help in pore refinement. The mix G20D0 followed by G10D10 performed the best among all the mixes at all curing days. Around 36.24%, 19.71%, 31.68%, 19.02%, and 12.09% increment in the pulse velocity is obtained at 7 curing days for the mixes G20D0, G15D5, G10D10, G5D15, and G0D20, respectively, in contrast to the control mix FA100 (2907 m/s) mix, as shown in Fig. 7. Moreover, the UPV improves as the number of curing days increases, indicating that the concrete gets better over time. At 28 curing days, the UPV value increased by 5.48%, 4.34%, 7.29%, 6.84%, 7.5%, and 6.26% for mixes FA100, G20D0, G15D5, G10D10, G5D15, and G0D20, respectively, when compared to the UPV value of each mix at 7 days of curing. Furthermore, rise of 39.743%, 24.64%, 39.16%, 21.64%, and 7.98% was spotted in pulse velocity for the mixes G20D0, G15D5, G10D10, G5D15, and G0D20, respectively, as compared to the control mix FA100 (3268.5 m/s) at 56 curing days. As concrete ages, the capillary pores and cracks are eliminated due to an

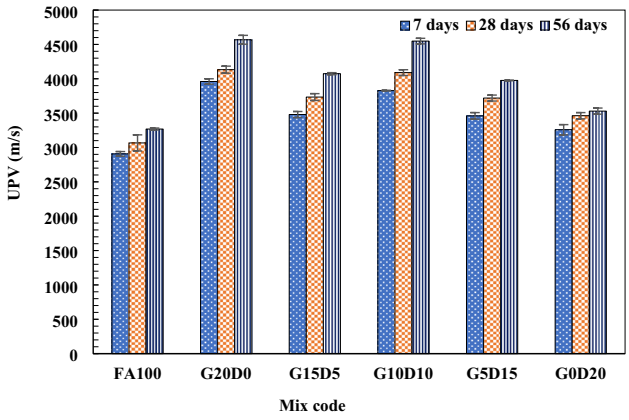

Fig. 7 UPV values of mixes at different curing days

increase in hydration, resulting in reduced pulse transmission resistance (Sadeghi Nik and Lotfi Omran 2013). The increase in UPV with age is a natural progression caused by the stiffening effect of the geopolymerization reaction. The quality of concrete increases from day to day for the same concrete samples due to geopolymerization, which makes it stronger and more durable over time.

4.7 Electrical resistivity

Electrical resistivity of all the GPC mixes has been measured to examine the effect of incorporation of various cementitious binders (GGBS and dolomite) in FA-based GPC. Overall, the addition of these binders as a partial replacement for FA has increased electrical resistivity at all curing ages. The overall trends as observed for the electrical resistivity of all the concrete mixes after 7, 28, and 56 days are presented in Fig. 8. The electrical resistivity in G20D0, G15D5, G10D10, G5D15, and G0D20 increased by 60.72%, 21.43%, 46.43%, 25%, and 17.86%, respectively, in comparison with FA100 (2.8 kΩ cm) at 7 days of curing. Similarly, at 28 and 56 curing days, the electrical resistivity further increases. Electrical resistivity values for mixes G20D0, G15D5, G10D10, G5D15, and G0D20 were found to increase by 67.65%, 35.29%, 47.06%, 20.58%, and 11.76%, respectively, after 28 days of curing and by 65%, 25%, 50%, 22.5%, and 7.5%, respectively, after 56 curing days, in comparison with the resistivity value of the control mix FA100 (3.4 kΩ cm at 28 days–4 kΩ cm at 56 days). Therefore, it can be inferred that the percentage of GGBS and dolomite in the concrete greatly influences the electrical resistivity values. Despite the higher electrical resistivity observed in mix G20D0, the results are quite comparable to that of mix G10D10 across all ages of curing. The fine GGBS and dolomite particles result in the densification of the concrete matrix, and hence fewer pores are available for saturation and movement of ions. Also, GGBS and dolomite have a larger specific surface area than

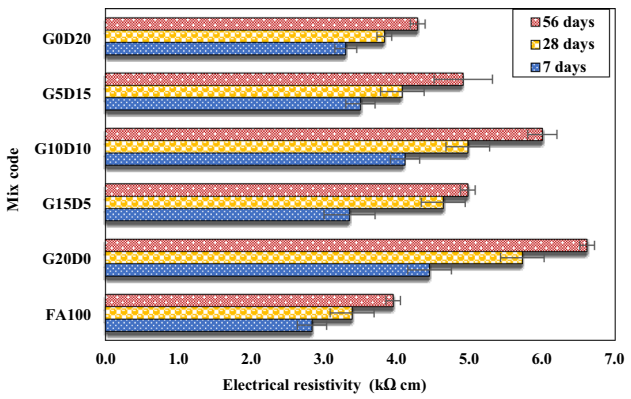

Fig. 8 Electrical resistivity values of mixes at different curing days

that of FA. This assertion can be substantiated by empirical evidences from the prior researches, where the specific surface area values of FA, GGBS, and dolomite have been reported as 385 m^2/kg (Liu et al. 2022), 400 m^2/kg (Yang et al. 2019), and 840 m^2/kg (Pehlivan et al. 2009), respectively. As a result, the geopolymerization products for these binders are much denser and more compact than geopolymers based on FA. However, as per AASHTO—T 358 (2015), the overall performance of all the mixes was not up to the mark as the resistivity values for all the mixes at all ages were less than 12 kΩ cm, indicating high chloride ion penetration.

4.8 Comparison of results with existing related literature

Table 4 summarizes the findings of several studies conducted by various authors, using different binder types (Bellum et al. 2022; Prabha et al. 2022; Verma and Dev 2022; Kumar and Reddy 2023). Previous researches indicate that using either GGBS or dolomite in FA-based GPC results in similar trends for mechanical and durability behaviors. However, no study has yet investigated the combined effect of both GGBS and dolomite in FA-based GPC. Additionally, there are very few investigations available that have examined the durability behavior, in terms of ISAT and CSAT. Furthermore, only a limited number of studies have examined non-destructive testing techniques, like UPV and electrical resistivity, for FA-based GPC containing GGBS and dolomite. As a result, the present study offers valuable insights into the performance of FA-based GPC containing both GGBS and dolomite, shedding light on its mechanical, durability, and non-destructive test properties.

4.9 ANOVA test

Significant values (i.e., P value) for the ANOVA test are presented in Table 5. Since the significant (P) value for both compressive strength and split tensile strength is smaller than 0.05, we have enough evidence to reject H_0 and accept H_1 (Vairagade et al. 2021). Therefore, it can be concluded that there is some significant difference between the six sets of mixes for a given number of days. The mix of various binders and its variants has a significant impact.

4.9.1 Reliability of strength

The significant variation in the mechanical strength, at 7, 28, and 56 curing days, due to the inclusion of different binders, is future studied and presented in Table 6. All the R^2 values are above 0.80, which provides good reliability

Table 4 Comparison of the present study results with the existing related literature

Authors	Binder type		Optimum replacement level (%)	Results (28 days)						
	Primary	Secondary		Slump value (mm)	Compressive strength (MPa)	Split tensile strength (MPa)	Initial surface absorption (ml/m^2 s)	Capillary suction absorption (mm/s$^{1/2}$)	Ultrasonic pulse velocity (m/s)	Electrical resistivity (kΩ cm)
Kumar and Reddy (2023)	FA	GGBS	40%	–	52.6	4.89	–	–	–	–
Verma and Dev (2022)	FA	GGBS	25%	–	32.1	4.6	–	–	4100	–
Prabha et al. (2022)	FA	Dolomite	20%	–	37.52	3.22	–	–	–	–
Bellum et al. (2022)	FA	GGBS	40%	55	50	8.4	–	0.003	–	–
Present study	FA	GGBS	20%	48	45.1	3.47	0.29	0.009	4132.5	5.7
Present study	FA	GGBS, Dolomite	10%, 10%	42	42.5	3.37	0.35	0.024	4090.0	5

Table 5 Significant values for ANOVA test

Statistics	Compressive strength (MPa)			Split tensile strength (MPa)		
	7 days	28 days	56 days	7 days	28 days	56 days
F statistics	7.998	15.099	16.546	27.159	26.063	20.062
P value	0.012	0.002	0.002	0.000	0.000	0.001
H_0 decision	Reject	Reject	Reject	Reject	Reject	Reject

of the mixes. Also, the value of standard error is very low, indicating the reliability of strength.

5 Cost analysis

The total cost for all six mixes is estimated and reported in Table 7 to determine the optimum mix obtained from the investigation. To estimate the cost, market prices for commercially available materials have been used. Cost is calculated for the quantity of material in kg/m^3. The G20D0 mix has been found to have the highest cost of Rs. 5928.95, followed by mix G15D5 (Rs. 5676.11). The control mix has been observed to have the lowest cost of all other mixes. Mixtures containing the percentage of dolomite, on the other hand, reduce costs significantly. The reduction of 4.2645%, 8.53%, 12.79%, and 17.06% has been observed for mixes G15D5, G10D10, G5D15, and G0D20, respectively, when compared to that of mix with maximum cost (G20D0). Hence, mix G10D10 can be a better substitute for mix G20D0 and mix G5D15 for mix G15D5 as their mechanical and durability properties are quite comparable.

6 Conclusions

This research emphasizes the potential of replacing FA with GGBS and dolomite to produce more eco-friendly and sustainable concrete. The study also validates the use of industrial waste as construction materials, addressing issues such as limited disposal sites and degrading environmental quality.

The incorporation of GGBS and dolomite has shown promising results in terms of improved mechanical strength, durability, sustainability, and environmental

Table 6 Regression statistics for reliability

Statistics	Compressive strength (MPa)			Split tensile strength (MPa)		
	7 days	28 days	56 days	7 days	28 days	56 days
R^2 value	0.854	0.813	0.821	0.885	0.853	0.870
Standard error	2.082	3.903	3.843	0.245	0.397	0.396
P value	0.002	0.006	0.005	0.019	0.031	0.023
T statistics	9.754	6.687	7.455	4.616	3.810	4.322

Table 7 Cost of materials and cost analysis of all the mixes

S. no.	Materials	Cost (Rs.)	Units
1	FA	163.93 (DSR)	cum
2	GGBS	12	kg
3	Dolomite	3.6	kg
4	NaOH	66	kg
5	Na_2SiO_3	19	kg
6	Coarse aggregate	90.8	cum
7	Fine aggregate	114.35	cum
8	SP	50	kg

Mix ID	FA (kg/m^3)	GGBS	Dolomite	Fine aggregate	Coarse aggregate	NaOH	Na_2SiO_3	SP	Cost (Rs.)
FA100	450	0	0	760.16	912.79	24.37	135	4.5	4497.65
G20D0	360	119.86	0	760.16	912.79	24.37	135	4.5	5928.95
G15D5	360	89.895	29.65	760.16	912.79	24.37	135	4.5	5676.11
G10D10	360	59.93	59.30	760.16	912.79	24.37	135	4.5	5423.27
G5D15	360	29.96	88.95	760.16	912.79	24.37	135	4.5	5170.43
G0D20	360	0	118.59	760.16	912.79	24.37	135	4.5	4917.58

friendliness of concrete. However, the inclusion of GGBS and dolomite in FA-based GPC as binder replacement significantly reduced the slump value. The asymmetrical shape and larger specific surface area of GGBS and dolomite particles compared to FA led to reduced workability and increased water demand. Dolomite, in particular, resulted in a greater decrease in workability due to its higher water demand.

Nevertheless, the addition of GGBS and dolomite significantly enhanced the compressive strength and split tensile strength of the GPC mixtures, at all curing ages. Incorporating 20% GGBS by weight of FA resulted in the highest strength gain of 66.2%, while a mix with 10% GGBS and 10% dolomite achieved a strength gain of 58.18% compared to the reference mix with 100% FA at 56 curing days. The higher calcium and silicate content of GGBS and dolomite accelerated the hydration rate, contributing to increased strength. The irregular shape of these particles also promoted mechanical anchoring within the concrete matrix, further enhancing strength.

Moreover, the inclusion of GGBS and dolomite reduced permeability and absorption rate, resulting in a denser microstructure with refined pore size and reduced surface absorption. The mixes containing 20% GGBS (i.e., G20D0) and 10% GGBS with 10% dolomite (i.e., G10D10) performed best in terms of permeability and absorption characteristics. The maximum reduction in IRA-SRA values of the order of 54.73–54.54% for mix G20D0 and 52.84–27.27% for G10D10 mix has been observed with respect to the control mix (0.0475–0.0011 $mm/s^{1/2}$).

Additionally, the mixes with GGBS and dolomite exhibited higher UPV values, indicating improved concrete densification and reduced pulse transmission resistance over time. As concrete ages, capillary pores and cracks are eliminated due to an increase in hydration, resulting in reduced pulse transmission resistance. The increase in UPV with age can be attributed to the stiffening effect due to the geopolymerization reaction. The overall electrical resistivity of the GPC mixes increased with the partial replacement of FA with GGBS and dolomite, indicating

reduced saturation and movement of ions due to the denser concrete matrix.

The results of the one-way ANOVA, conducted to assess the compressive and split tensile strength at various curing days, demonstrated significant variation among the mixes. Moreover, the R^2 values being consistently above 0.80 indicated a high level of reliability for the mixes.

In terms of cost, the research indicates that the mix with 10% GGBS and 10% dolomite provides a more cost-effective solution compared to the mix with 20% GGBS, as it achieved comparable mechanical and durability properties while reducing costs by 8.53%. These findings demonstrate the potential and benefits of utilizing GGBS and dolomite as sustainable alternatives in GPC for various civil engineering applications.

Acknowledgements The authors extend their sincere appreciation to the Department of Civil Engineering, Dr B R Ambedkar National Institute of Technology, Jalandhar, for their invaluable support and access to state-of-the-art laboratory facilities.

Funding No funding was received to assist with the preparation of this manuscript.

Declarations

Conflict of interest The authors have no competing interests to declare that are relevant to the content of this article.

Ethical approval It has been confirmed that the work is original and has not been published elsewhere, nor is it currently under consideration for publication elsewhere in any form or language (partially or in full), and its publication has been approved by all coauthors.

References

Abdul Aleem MI, Arumairaj PD (2012) Geopolymer concrete—a review. Int J Eng Sci Emerg Technol 1:118–122. https://doi.org/10.7323/ijeset/v1

Adediji YB, Adeyinka AM, Yahya DI, Mbelu OV (2023) A review of energy storage applications of lead-free $BaTiO_3$-based dielectric ceramic capacitors. Energy Ecol Environ. https://doi.org/10.1007/s40974-023-00286-5

Agrawal Y, Gupta T, Siddique S, Sharma RK (2021) Potential of dolomite industrial waste as construction material: a review. Innov Infrastruct Solut 6:1–15. https://doi.org/10.1007/s41062-021-00570-5

Ahmed HU, Mohammed AS, Faraj RH et al (2022) Compressive strength of geopolymer concrete modified with nano-silica: experimental and modeling investigations. Case Stud Constr Mater 16:e01036. https://doi.org/10.1016/j.cscm.2022.e01036

Albitar M, Mohamed Ali MS, Visintin P, Drechsler M (2017) Durability evaluation of geopolymer and conventional concretes. Constr Build Mater 136:374–385. https://doi.org/10.1016/j.conbuildmat.2017.01.056

Ambikakumari Sanalkumar KU, Yang E-H (2021) Self-cleaning performance of nano-TiO_2 modified metakaolin-based geopolymers. Cem Concr Compos 115:103847. https://doi.org/10.1016/j.cemconcomp.2020.103847

Asghar R, Khan MA, Alyousef R et al (2023) Promoting the green construction: scientometric review on the mechanical and structural performance of geopolymer concrete. Constr Build Mater 368:130502. https://doi.org/10.1016/j.conbuildmat.2023.130502

ASTM C1585-13 (2013) Standard test method for measurement of rate of absorption of water by hydraulic cement concretes. ASTM Int 41:1–6

Barbhuiya S (2011) Effects of fly ash and dolomite powder on the properties of self-compacting concrete. Constr Build Mater 25:3301–3305. https://doi.org/10.1016/j.conbuildmat.2011.03.018

Bellum RR, Al Khazaleh M, Pilla RK et al (2022) Effect of slag on strength, durability and microstructural characteristics of fly ash-based geopolymer concrete. J Build Pathol Rehabil 7:1–15. https://doi.org/10.1007/s41024-022-00163-4

Bhatt A, Priyadarshini S, Acharath Mohanakrishnan A et al (2019) Physical, chemical, and geotechnical properties of coal fly ash: a global review. Case Stud Constr Mater 11:e00263. https://doi.org/10.1016/j.cscm.2019.e00263

Bostanci ŞC, Limbachiya M, Kew H (2016) Portland slag and composites cement concretes: engineering and durability properties. J Clean Prod 112:542–552. https://doi.org/10.1016/j.jclepro.2015.08.070

BS1881-208 (1996) Recommendations for the determination of the initial surface absorption of concrete. Br Stand 2:1–14

Buchwald A, Hilbig H, Kaps C (2007) Alkali-activated metakaolin-slag blends—performance and structure in dependence of their composition. J Mater Sci 42:3024–3032. https://doi.org/10.1007/s10853-006-0525-6

Cohen E, Peled A, Bar-Nes G (2019) Dolomite-based quarry-dust as a substitute for fly-ash geopolymers and cement pastes. J Clean Prod 235:910–919. https://doi.org/10.1016/j.jclepro.2019.06.261

CPWD (2021) Delhi schedule of rates (DSR)

Davidovits J (1994) Global warming impact on the cement and aggregates industries. World Resour Rev 6:263–278

Davidovits J (2013) Geopolymer cement a review. Geopolym Sci Tech 21:1–11

Davidovits J (1999) Chemistry of geopolymeric systems, terminology. In: Proceedings of geopolymer international conference Fr 99

Dimas D, Giannopoulou I, Panias D (2009) Polymerization in sodium silicate solutions: a fundamental process in geopolymerization technology. J Mater Sci 44:3719–3730. https://doi.org/10.1007/s10853-009-3497-5

Eisa M, Ragauskaitė D, Adhikari S et al (2022) Role and responsibility of sustainable chemistry and engineering in providing Safe and sufficient nitrogen fertilizer supply at turbulent times. ACS Sustain Chem Eng 10:8997–9001. https://doi.org/10.1021/acssuschemeng.2c03972

Farooq M, Krishna A, Banthia N (2022) Highly ductile fiber reinforced geopolymers under tensile impact. Cem Concr Compos 126:104374. https://doi.org/10.1016/j.cemconcomp.2021.104374

Fonseca M, Matos AM (2023) 3D construction printing standing for sustainability and circularity: material-level opportunities. Materials (basel). https://doi.org/10.3390/ma16062458

Gandolfo M, Amici J, Fagiolari L et al (2022) Designing photocured macromolecular matrices for stable potassium batteries. Sustain Mater Technol 34:e00504. https://doi.org/10.1016/j.susmat.2022.e00504

Gill P, Jangra P, Ashish DK (2023) Non-destructive prediction of strength of geopolymer concrete employing lightweight recycled aggregates and copper slag. Energy Ecol Environ. https://doi.org/10.1007/s40974-023-00281-w

Howladar MF, Islam MR (2016) A study on physico-chemical properties and uses of coal ash of Barapukuria coal fired thermal power plant, Dinajpur, for environmental sustainability. Energy Ecol Environ 1:233–247. https://doi.org/10.1007/s40974-016-0022-y

Ibrahim WMW, Abdullah MMAB, Ahmad R et al (2022) Chemical distributions of different sodium hydroxide molarities on fly ash/dolomite-based geopolymer. Materials (basel). https://doi.org/10.3390/ma15176163

IS 1199 (1959) Methods of sampling and analysis of concrete. Bur Indian Stand, pp 1–49

IS:12089–1987 (1987) Specification for granulated slag for the manufacture of Portland slag cement. Bur Indian Stand New Delhi, pp 1–14

IS: 3812 (Part-1) (2003) Pulverized fuel ash—specification. Part 1: for use as Pozzolana in cement, cement mortar and concrete (Second Revision). Bur Indian Stand, pp 1–14

IS 516 (1959) Method of tests for strength of concrete. Bur Indian Stand, pp 1–30

IS 516: Part 5 (Section 1) (2018) Hardened concrete—methods of test-testing of strength of hardened concrete. Bur Indian Stand New Delhi

IS 5816 (1999) Indian standard splitting tensile strength of concrete-method of test (first revision). Bur Indian Stand New Delhi (reaffirme:1–14)

Junaid TM, Kayali O, Khennane A (2017) Response of alkali activated low calcium fly-ash based geopolymer concrete under compressive load at elevated temperatures. Mater Struct Constr. https://doi.org/10.1617/s11527-016-0877-6

Kajaste R, Hurme M (2016) Cement industry greenhouse gas emissions—management options and abatement cost. J Clean Prod 112:4041–4052. https://doi.org/10.1016/j.jclepro.2015.07.055

Kumar NLNK, Reddy IVR (2023) Parametric studies on the fresh, mechanical and microstructural properties of GGBS blended self compacting geopolymer concrete cured under ambient condition. J Build Pathol Rehabil. https://doi.org/10.1007/s41024-023-00332-z

Liang G, Liu T, Li H, Wu K (2022) Shrinkage mitigation, strength enhancement and microstructure improvement of alkali-activated slag/fly ash binders by ultrafine waste concrete powder. Compos Part B Eng 231:109570. https://doi.org/10.1016/j.compositesb.2021.109570

Liu MYJ, Alengaram UJ, Santhanam M et al (2016) Microstructural investigations of palm oil fuel ash and fly ash based binders in lightweight aggregate foamed geopolymer concrete. Constr Build Mater 120:112–122. https://doi.org/10.1016/j.conbuildmat.2016.05.076

Liu Y, Hao W, He W et al (2022) Influence of dolomite rock powder and iron tailings powder on the electrical resistivity, strength and microstructure of cement pastes and concrete. Coatings 12:1–14. https://doi.org/10.3390/coatings12010095

Malhotra VM (2002) Introduction: sustainable development and concrete technology. ACI Concr Int 24:22

Nath P, Sarker PK (2015) Use of OPC to improve setting and early strength properties of low calcium fly ash geopolymer concrete cured at room temperature. Cem Concr Compos 55:205–214. https://doi.org/10.1016/j.cemconcomp.2014.08.008

Pasupathy K, Berndt M, Sanjayan J et al (2017) Durability of low-calcium fly ash based geopolymer concrete culvert in a saline environment. Cem Concr Res 100:297–310. https://doi.org/10.1016/j.cemconres.2017.07.010

Patankar SV, Ghugal YM, Jamkar SS (2015) Mix design of fly ash based geopolymer concrete. Advances in structural engineering. Springer India, New Delhi, pp 1619–1634

Patel YJ, Shah N (2018) Enhancement of the properties of ground granulated blast furnace slag based self compacting geopolymer concrete by incorporating rice husk ash. Constr Build Mater 171:654–662. https://doi.org/10.1016/j.conbuildmat.2018.03.166

Pavithra P, Srinivasula Reddy M, Dinakar P et al (2016) A mix design procedure for geopolymer concrete with fly ash. J Clean Prod 133:117–125. https://doi.org/10.1016/j.jclepro.2016.05.041

Pehlivan E, Müjdat A, Dinc S (2009) Adsorption of Cu^{2+} and Pb^{2+} ion on dolomite powder. J Hazard Mater 167:1044–1049. https://doi.org/10.1016/j.jhazmat.2009.01.096

Pirrone N, Bella F, Hernández S (2022) Solar H2 production systems: current status and prospective applications. Green Chem 24:5379–5402. https://doi.org/10.1039/d2gc00292b

Prabha VC, Revathi V, Sivamurthy Reddy S (2022) Ambient cured high calcium fly ash geopolymer concrete with dolomite powder. Eur J Environ Civ Eng 26:7857–7877. https://doi.org/10.1080/19648189.2021.2012262

Provis JL (2014) Geopolymers and other alkali activated materials: Why, how, and what? Mater Struct Constr 47:11–25. https://doi.org/10.1617/s11527-013-0211-5

Purushotham P, Prasad MH, Naveen P (2017) A study on green concrete. Int Res J Eng Technol 04:601–607

Qu F, Li W, Tao Z et al (2020) High temperature resistance of fly ash/GGBFS-based geopolymer mortar with load-induced damage. Mater Struct Constr. https://doi.org/10.1617/s11527-020-01544-2

Radahakrishnan S, Selvan KG, Kumar SS (2017) Geo polymer in construction. Bus Stud (IJRMBS 2017) 4:3–5

Ramineni K, Boppana NK, Ramineni M (2018) Performance studies on self-compacting geopolymer concrete at ambient curing condition. In international congress on polymers in concrete (ICPIC 2018), pp 501–508. https://doi.org/10.1007/978-3-319-78175-4_64

Reddy MS, Dinakar P, Rao BH (2018) Mix design development of fly ash and ground granulated blast furnace slag based geopolymer concrete. J Build Eng 20:712–722. https://doi.org/10.1016/j.jobe.2018.09.010

Sadeghi Nik A, Lotfi Omran O (2013) Estimation of compressive strength of self-compacted concrete with fibers consisting nano-SiO_2 using ultrasonic pulse velocity. Constr Build Mater 44:654–662. https://doi.org/10.1016/j.conbuildmat.2013.03.082

Saranya P, Nagarajan P, Shashikala AP (2019) Development of ground-granulated blast-furnace slag-dolomite geopolymer concrete. ACI Mater J 116:235–243. https://doi.org/10.14359/51716981

Schmitz F, Lago N, Fagiolari L et al (2022) High open-circuit voltage $Cs_2AgBiBr_6$ carbon-based perovskite solar cells via green processing of ultrasonic spray-coated carbon electrodes from waste tire sources. Chemsuschem. https://doi.org/10.1002/cssc.202201590

Sharma A, Basumatary N, Singh P et al (2022a) Potential of geopolymer concrete as substitution for conventional concrete: a review. Mater Today Proc 57:1539–1545. https://doi.org/10.1016/j.matpr.2021.12.159

Sharma A, Singh P, Kapoor K (2022b) Utilization of recycled fine powder as an activator in fly ash based geopolymer mortar. Constr Build Mater 323:126581. https://doi.org/10.1016/j.conbuildmat.2022.126581

Singh GVPB, Subramaniam KVL (2019) Influence of processing temperature on the reaction product and strength gain in alkali-activated fly ash. Cem Concr Compos 95:10–18. https://doi.org/10.1016/j.cemconcomp.2018.10.010

Singh N, Singh A, Ankur N et al (2022) Reviewing the properties of recycled concrete aggregates and iron slag in concrete. J Build Eng 60:105150. https://doi.org/10.1016/j.jobe.2022.105150

Singh RP, Vanapalli KR, Cheela VRS et al (2023) Fly ash, GGBS, and silica fume based geopolymer concrete with recycled aggregates: properties and environmental impacts. Constr Build Mater 378:131168. https://doi.org/10.1016/j.conbuildmat.2023.131168

Standard I (2016) Coarse and fine aggregate for concrete—specification (Third Revision) IS383. p 19

Švajlenka J, Pošiváková T (2023) Innovation potential of wood constructions in the context of sustainability and efficiency of the construction industry. J Clean Prod. https://doi.org/10.1016/j.jclepro.2023.137209

T 358 (2015) AASHTO T 358 Surface resistivity indication of concrete's ability to resist chloride ion penetration. AASHTO. Am Assoc State Highw Transp Off

Thakur M, Bawa S (2022) Self-compacting geopolymer concrete: a review. Mater Today Proc 59:1683–1693. https://doi.org/10.1016/j.matpr.2022.03.400

Vairagade VS, Uparkar SS, Lokhande KG et al (2021) A numerical analysis of green sustainable concrete using ANOVA. Turk J Comput Math Educ 12:4605–4612

Verma M, Dev N (2022) Effect of ground granulated blast furnace slag and fly ash ratio and the curing conditions on the mechanical properties of geopolymer concrete. Struct Concr 23:2015–2029. https://doi.org/10.1002/suco.202000536

Wong LS (2022) Durability performance of geopolymer concrete: a review. Polymers (basel). https://doi.org/10.3390/polym14050868

Yang J, Huang J, He X et al (2019) Segmented fractal pore structure covering nano-and micro-ranges in cementing composites produced with GGBS. Constr Build Mater 225:1170–1182. https://doi.org/10.1016/j.conbuildmat.2019.08.016

Ye H, Fu C, Yang G (2019) Influence of dolomite on the properties and microstructure of alkali-activated slag with and without pulverized fly ash. Cem Concr Compos 103:224–232. https://doi.org/10.1016/j.cemconcomp.2019.05.011

Yip CK, Lukey GC, Van Deventer JSJ (2005) The coexistence of geopolymeric gel and calcium silicate hydrate at the early stage of alkaline activation. Cem Concr Res 35:1688–1697. https://doi.org/10.1016/j.cemconres.2004.10.042

Zhao X, Liu C, Wang L et al (2019) Physical and mechanical properties and micro characteristics of fly ash-based geopolymers incorporating soda residue. Cem Concr Compos 98:125–136. https://doi.org/10.1016/j.cemconcomp.2019.02.009